# Torque Measurements and DEM Simulations in a Cuette-type Device with Application to Particle Size Measurements

B. Dencs[1], J. Szepvolgyi[1], G. I. Tardos[2] and J. Gyenis[1]

[1] University of Kaposvar, Research Institute of Chemical & Process Engineering, Egyetem u. 2, H-8200, Veszprem, Hungary

[2] The City College of the City University of New York, Department of Chemical Engineering, Convent Ave. and 140 Street, New York, NY 10031, USA

## Abstract

A continuously operating modified Cuette-type shearing device has been developed for *in-situ* measurements to estimate the average particle size during size enlargement processes in fluidized bed granulator. It was proven by experiments that well-defined correlation exists between the mean torque and the average particle size being in the device. DEM simulations revealed interesting aspects of this method.

*Key words*: granular flow, torque measurement, particle size, Cuette device, simulation

## 1. Introduction

During granulation or size enlargement processes, one of the most important features of the treated solids is particle size. There are a number of different methods and devices to measure and control the size and size distribution of the product. These can be used on- or off-line, in situ or employing separate measuring tools. One of these methods is based on force measurements during continuous shearing of particle bed, carried out in a Cuette-type shearing device. To study the forces acting on a slowly rotating rough cylinder in a dry frictional powder, Tardos and co-workers [1] used such a piece of equipment (see Fig.1). During the work reported here, this type of device was used to estimate the actual particle size during a size enlargement process. Other workers [3-4] also used similar devices for continuous shearing of fine fluidized powders.

During this work, a Cuette-type device was applied in a special fluidized-bed granulator, which recovers solids directly from solutions or suspensions [5]. In such equipment, shown in *Fig.2*, a constant and narrow size distribution can be achieved by ensuring equilibrium between the effects of simultaneous attrition and granulation. Attrition of larger granules in this equipment takes place due to the breaking effect of notched grinding rolls rotating and orbiting along the wall of the equipment. At the same time, the size enlargement of smaller particles is the consequence of simultaneous agglomeration and surface layering due to spraying solution of binding material into the particle bed. On-line size measurement may help to control the equilibrium granule size during these concurrent processes, by setting the operational parameters to appropriate values. Details of the operation of this equipment can be found elsewhere [5].

## 2. Experimental

For the present work, a modified Cuette-type device (*Fig.3*), similar to that employed by Tardos et al. [1, 2] was used to study the effect of particle size on the measured torque during continuous shearing of dry, granulated sucrose particles.

The experimental device consisted of an inner rotating, and an outer stationary cylinder.

Both were covered by coarse sandpaper to ensure that wall friction be comparable to the internal friction of the particle bed. The inner cylinder could be rotated between $n=60$ and $240$ RPM ($v_p=0.16-0.65$ m/s peripheral speed) by an electronically controlled DC motor. The torque was continuously measured and recorded by a data acquisition system connected to a PC. The maximum measurable torque was $0.44$ N-m.

The diameters of the outer stationary cylinder and that of the inner rotating cylinder were $D=106$ mm and $D_c=52$ mm, respectively. Thus, the width of the gap between the two cylinders was $l_g=26$ mm. This gap was about two times wider, compared to the earlier experiments of Tardos et al. [2], thus the shear region do not extended to the wall of the outer standing cylinder. The heights of the particle bed and the rotating cylinder were $100$ mm and $80$ mm, respectively.

The main characteristics of the granular material prepared from sucrose by granulation used for the experiments are given in *Table 1*. The mean particle sizes were varied between $d=0.3$ and $1.4$ mm.

*Table 1. Characteristics of the particles*

|  | Sucrose size range mm | Sucrose mean particle size mm | Form of particles | Angle of repose | Flowability $cm^3/s$ | Bulk density $kg/m^3$ |
|---|---|---|---|---|---|---|
| 1 | 0.20-0.40 | 0.30 | prismatic* | 39.0 | 13.3 | 740 |
| 2 | 0.40-0.63 | 0.52 | prismatic* | 39.1 | 12.8 | 760 |
| 3 | 0.63-0.80 | 0.72 | rounded prism | 39.8 | 11.9 | 770 |
| 4 | 0.80-1.00 | 0.90 | near spherical | 40.9 | 11.0 | 760 |
| 5 | 1.25-1.60 | 1.43 | near spherical | 40.9 | 8.9 | 790 |

* without sharp tips and edges

## 3. Results and discussion

The curves, shown in *Fig.4*, represent typical torque signals obtained for five different mean particle sizes (*0.30, 0.52, 0.72, 0.9, 1.43 mm* respectively). The sixth curve near the bottom refers to the torque measured in the empty device, i.e. with no particles. This represents only the friction of bearings and a small brake force that was necessary to adjust the basic level of torque. During evaluation, this latter value was subtracted from all measured torque data. From this Figure, it is evident that, after a short initial transient period, the mean value of the measured torque signals remained essentially constant with some stochastic fluctuations.

As seen from *Fig.5*, the mean value of the torque increases with the mean particle size, for different rotation speeds (*n=80 and 120 rpm*) and for different preset break forces. This dependence was more pronounced at lower rotation speed, especially below $d=0.8$-$0.9$ mm granule diameters for the given geometry and design of the measuring device. The preset break force (i.e. the basic level of torque) had no significant influence.

Measurements were also performed with particles moving downwards within the gap between the cylinders. A sliding velocity of $v_s=0.001$m/s, corresponding to *2.0-2.2 kg/h* mass flow rate of particles was chosen to be negligibly small, relatively to the $v_p=0.22$ *m/s* peripheral velocity of the rotating cylinder. This sliding velocity ensured continuous replacement of the material being in the measuring cell with not too long time delay. It was resulted that this vertical motion had no observable influence on the torque values.

Experiments were also performed with particle systems having much broader size distribution compared to the narrow granule fractions given in *Table 1*. Two particle

systems with broad size distribution were tested in this respect. One of them was blended from the first three fractions of *Table 1*, resulting in a size distribution between *d=0.20-0.63 mm* and *d=0.45 mm* mean particle size. By blending the last two particle fractions of *Table 1*, *d=0.63-1.60 mm* size distribution and *1.1 mm* mean particle size was obtained. The results of torque measurements are shown in *Fig.6*. From this, it became evident that torque values obtained by these fractions did not show broader scattering than obtained for the narrow particle size distributions. Deviation between the real mean particle sizes and those calculated from torque values remained below 10 per cent.

To simulate experimentally the transition from one particle size to another in a continuously working granulator, sucrose particles with *d=0.40-0.63 mm* size range (mean particle size *0.52 mm*) were initially filled into the fluidized bed. The modified Cuette-type device was connected to the granulator as shown in *Fig.7*. Continuous flow of particles was ensured through the measuring cell by a screw feeder with $v_s=0.001$ m/s superficial velocity. Subsequently, larger particles with *d=0.80-1.00 mm* size range (mean particle size *0.90 mm*) were continuously introduced into the fluidized bed, and the torque was continuously measured and recorded. The mean particle sizes calculated from these torque values are plotted in *Fig.8* for about *800 s* period. To check the reliability of this method, mean particle size in the granulator was measured at the beginning and at the end of the measuring period by sieve analysis. It is clearly seen from this Figure that the transition from the smaller mean particle size to the larger one could be monitored by this method with appropriate accuracy. Deviation between the data calculated from torque signals and measured by sieve analysis was below 8%.

To compare these results to earlier theory and experiments, some discussion is needed. Tardos et al. [1, 2] proposed the following general expression to evaluate this kind of experimental data

$$M_q = \pi \rho_B g L^2 R^2 \sin\phi \left[ 1 - \frac{U}{U_{mf}} \right] \qquad (1)$$

According to this equation, the torque $M_q$ is proportional to $L^2$ and $R^2$ (where $L$ and $R$ are the height of the sheared layer and the radius of the inner cylinder, respectively). Linear dependence is found on bulk density $\rho_B$, on the inner friction coefficient of the particle bed, *sinΦ*, and on (1-$U$/$U_{mf}$), where $U$ and $U_{mf}$ are the actual superficial gas velocity and the minimum fluidization velocity, respectively. However, no direct relation is shown with particle diameter.

There is no clear explanation of the discrepancy between the experimental findings where torque depended on particle size and the above equation where there is no dependence. It is true that *Eqn.1* was obtained for shearing particle beds in a relatively narrow gap between the surfaces of the stationary and rotating cylinders. In this case, the effect of shear has extended over the whole particle region in the gap, from the inner rotating to the outer stationary wall, independently of particle size. But, in the experiments presented here, much wider gaps were used between the two cylinders. Therefore, the torque measured on the shaft of the rotation cylinder might depend on friction forces between the moving and stationary particle regions, which in turn could be influenced by the sizes of the particles and geometric parameters. This possible explanation was supported by DEM simulation.

### DEM simulation

DEM (Distinct Element Modeling) simulation, based on the method developed and applied to a number of systems by Tsuji et al. [6], was carried out for the particle system

and Cuette-type device used for the experiments. By this way, both the instantaneous position and velocity of all particles could be determined, as well as the direction and magnitude of forces acting on them. By summing of the tangential forces along a given cylindrical surface within the sheared particle bed, the friction acting against rotation could be calculated.

*Fig.9* shows snapshots on the positions of particles in a cross section of the simulated Cuette device at different time intervals (*t=0.0, 0.4, 0.8 and 1.2 s*). From this, it is clearly seen that particles which, directly or indirectly, get into contact with the rotating surface are moving in the same direction as the inner cylinder (but with lower velocity due to the slip between them). *Fig.10* shows the mean angular velocity of particles, for three different particle diameters as a function of their distance from the center of rotation, i.e. from the axis of the rotating cylinder. These plots show decaying angular velocity as the distance from the cylinder surface increases.

*Fig.11* shows the time signal of the summarized frictional forces acting on the particles situated in the particle layer adjacent to the surface of the rotating cylinder. Averages of these time signals after achieving quasi steady state conditions are plotted vs. particle diameter in *Fig.12*. The tendency is very similar to that obtained by the experiments: the shear forces between the surface of the rotating cylinder and the contacting particles are increasing as the particle diameter is increasing. It means that these results seem to confirm the experimental findings and give an explanation of the measured behavior.

## 4. Conclusions

A modified Cuette-type shearing device with a relatively small rotating inner cylinder and wide gap for the sheared particle bed was constructed. The effect of particle size on the torque acting on the shaft of the driving motor was studied. For five different sucrose particle fractions with mean diameters ranging from *0.3* to *1.4 mm*, it was observed that the measured torque has significantly increased as a function of the mean particle size. This finding was also validated for sliding particle beds and for broader size distribution. This method could also be applied under non steady-state conditions.

**References**

1. Tardos, G. I., Khan, M. I., Schaeffer, D. G.: Forces on a slowly rotating rough cylinder in a Couette device containing a dry, frictional powder. *Physics of Fluids,* **10** (2) (1998) 335.

2. Tardos, G. I., Khan, M. I., Mort, P. R.: Critical parameters and limiting conditions in binder granulation of fine powders. *Powder Technol.,* **94** (1997) 245.

3. Cheremisinoff, N. P., Cheremisinoff, P. N.: Hydrodynamics of Gas-Fluid Fluidization, Gulf, Houston, Texas, 1984, 127.

4. Anjaneyulu P., Khakhar D.V.: Rheology of a gas-fluidized bed. *Powder Technol.* **83** (1995) 29.

5. Dencs, B., Ormós, Z.: Particle size control in fluidized bed spray-dryer and granulator during the recovery of solids from liquids. *Hung. J. Ind. Chem.,* **21** (1993) 225.

6. Tsuji, Y.: Discrete Particle Simulation of Gas-Solids Flows (From Dilute to Dense Flow) Review, *KONA*, **57** (1993) 11.
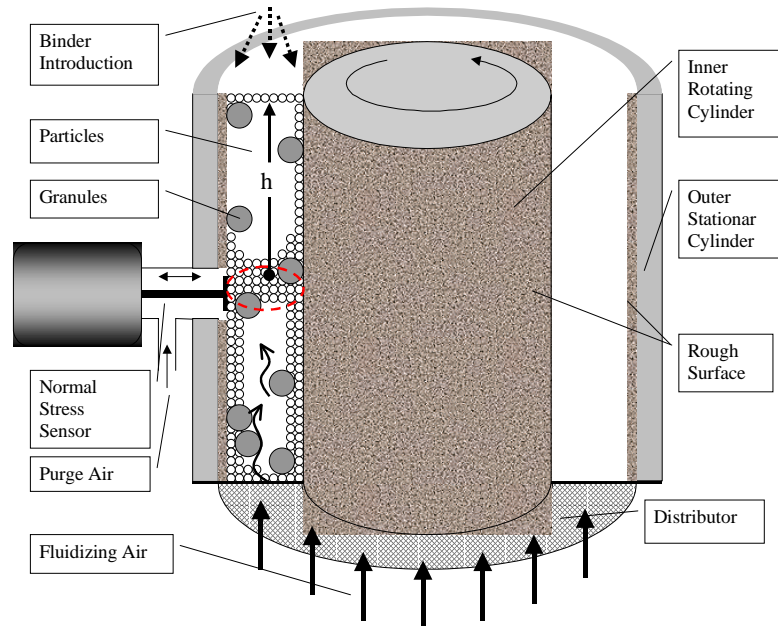
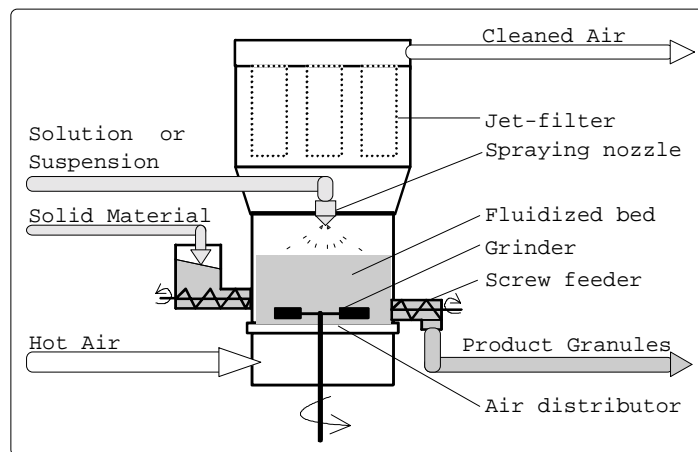Figure 1. Schematic diagram of the Cuette-shearing device used by Tardos et al. [2]



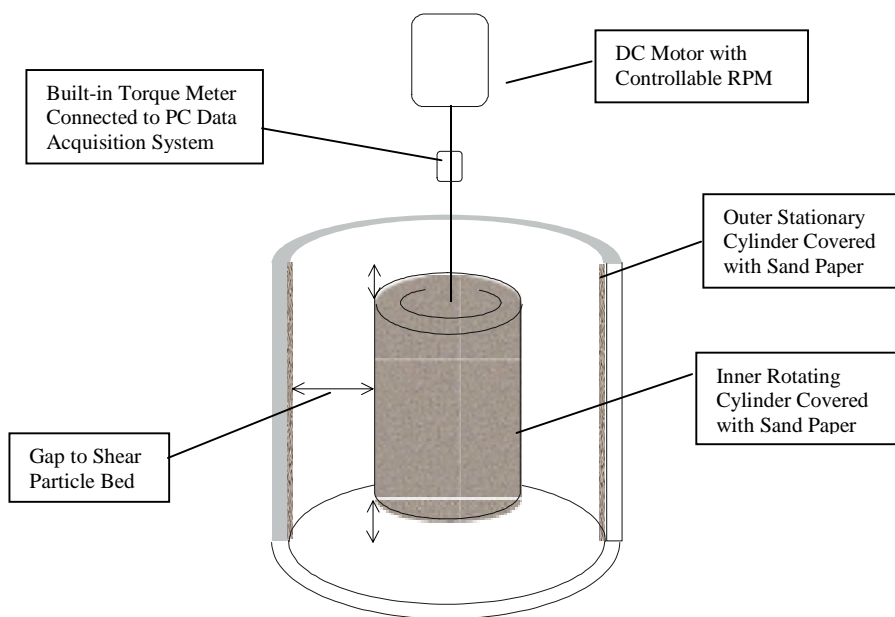Figure 2. Schematic diagram of a continuously operating grinding granulator [3]



Figure 3. Schematic diagram of the modified Cuette device used for these experiments
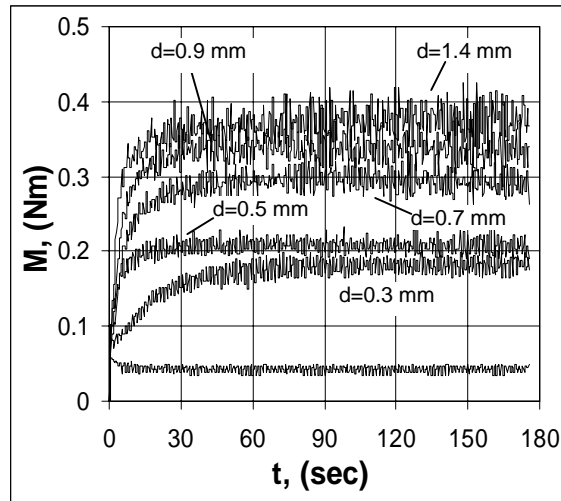
Figure 4. Torque signals versus time measured with different mean particle sizes
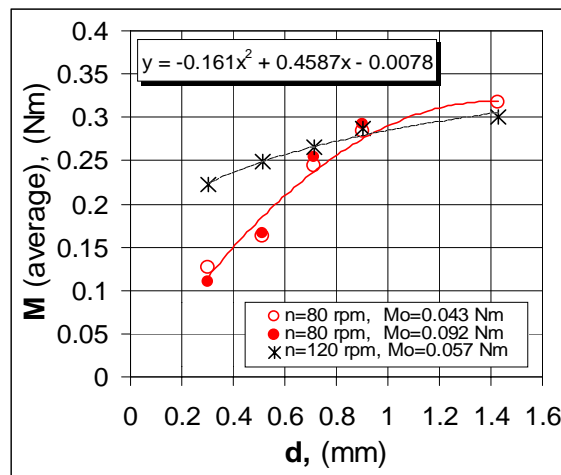


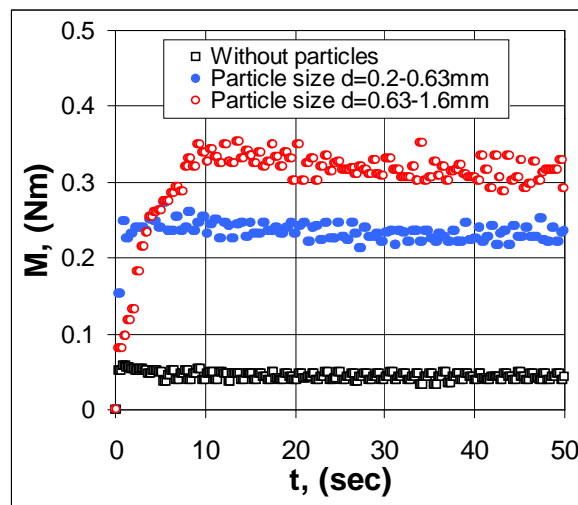Figure 5. Average torque values versus mean particle size



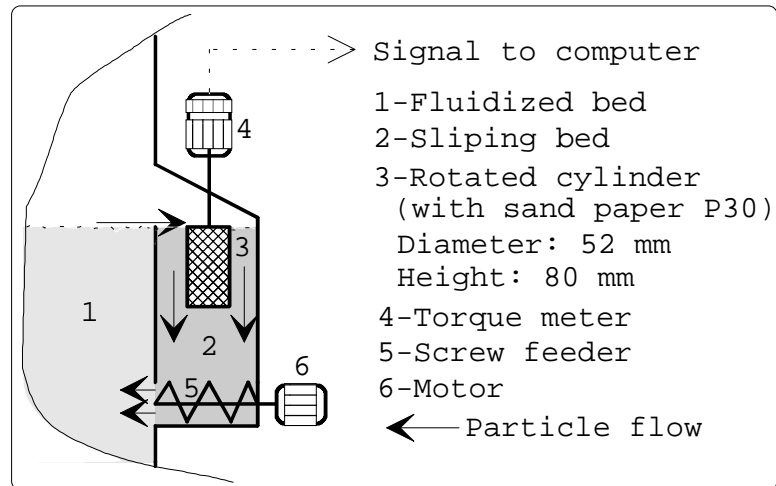Figure 6. Average torque values measured versus time for a broad size distribution

Figure 7. Cuette-type measuring cell, connected to fluidized bed granulator
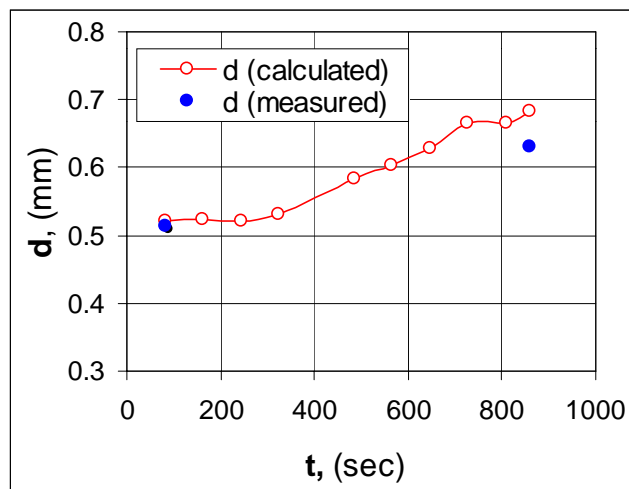


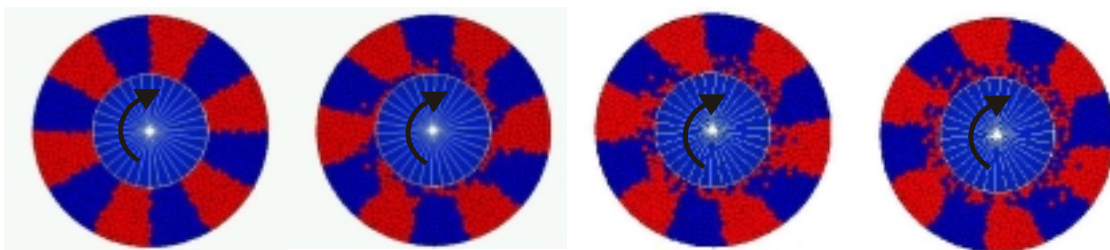Figure 8. Transition of particle size data calculated from torque values



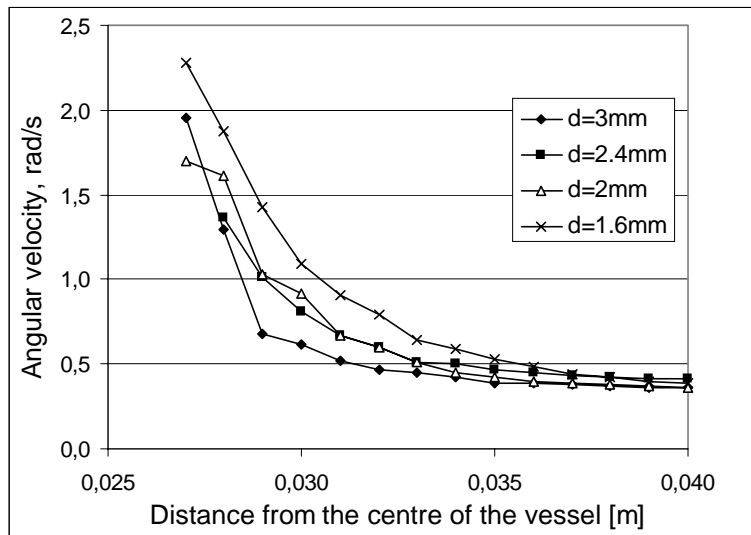Figure 9. Snapshots of particle positions during shearing of the particle bed

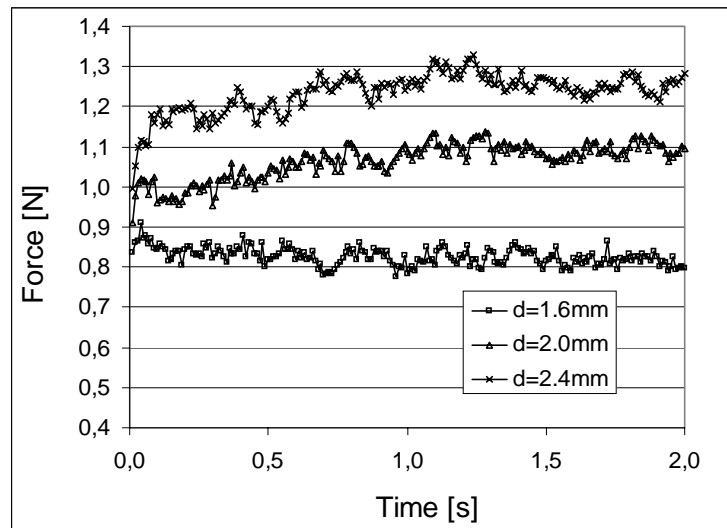Figure 10. Average angular velocity of particles around the inner cylinder



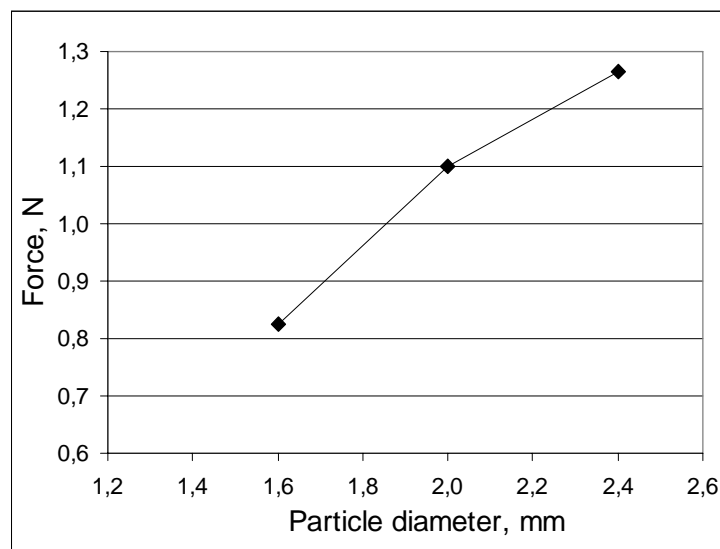Figure 11. Tangential frictional forces acting on the particles around the rotating cylinder



Figure 12. Average of frictional forces as a function of particle diameter